RESEARCH ARTICLE

Optimal dose reduction algorithm using an attenuation-based tube current modulation method for cone-beam CT imaging

Kihong Son[1], Jieun Chang[1], Hoyeon Lee[1], Changhwan Kim[1], Taewon Lee[1], Seungryong Cho[1], Sohyun Park[2], Jin Sung Kim[2]*

1 Department of Nuclear and Quantum Engineering, Korea Advanced Institute of Science and Technology, Daejeon, Korea, **2** Department of Radiation Oncology, Yonsei Cancer Center, Yonsei University College of Medicine, Yonsei University Health System, Seoul, Korea

* jinsung.k@gmail.com

Abstract

To reduce the radiation dose given to patients, a tube current modulation (TCM) method has been widely used in diagnostic CT systems. However, the TCM method has not yet been applied to a kV-CBCT system on a LINAC machine. The purpose of this study is to investigate if a TCM method would be desirable in a kV-CBCT system for image-guided radiation therapy (IGRT) or not. We have developed an attenuation–based TCM method using prior knowledge from planning CT images of patients. The TCM method can provide optimized dose reductions without degrading image quality for kV-CBCT imaging. Here, we investigate whether or not our suggested TCM method is desirable to use in kV-CBCT systems to confirm and revise the exact position of a patient for IGRT. Patients go through diagnostic CT scans for RT planning; therefore, using information from prior CT images can enable estimations of the total X-ray attenuation through a patient's body in a CBCT setting for radiation treatment. Having this planning CT image allows to use the proposed TCM method in RT. The proposed TCM method provides a minimal amount of current for each projection, as well as total current, required to reconstruct the current modulated CBCT image with an image quality similar to that of CBCT. After applying a calculated TCM current for each projection, projection images were acquired and the current modulated CBCT image was reconstructed using a FDK algorithm. To validate the proposed approach, we used a numerical XCAT phantom and a real ATOM phantom and evaluated the performance of the proposed method via visual and quantitative image quality metrics. The organ dose due to imaging radiation was calculated in both cases and compared using the GATE simulation toolkit. As shown in the quantitative evaluation, normalized noise and SSIM values of the TCM were similar to those of conventional CBCT images. In addition, the proposed TCM method yielded comparable image quality to that of conventional CBCT images for both simulations and experimental studies as organ doses were decreased. We have successfully demonstrated the feasibility and dosimetric merit of a prototypical TCM method for kV-CBCT via simulations and experimental study. The results indicate that the proposed TCM method and overall framework can be a viable option for CBCT imaging that utilizes an

optimal dose reduction without degrading image quality. Thus, this method reduces the probability for side effects due to radiation exposure.

Introduction

Image-guided radiation therapy (IGRT) has been extensively used for target localization, patient positioning, and external beam adjustment in radiation therapy procedures [1]. One approach of IGRT is kV cone-beam computed tomography (CBCT), which is used to get a patient's anatomy before treatment [1, 2]. In practice, kV-CBCT imaging enables technicians and doctors to observe the target and position of organs at risk before treatment while the patient is on the couch. However, repeated use of kV-CBCT has raised concerns regarding radiosensitive organs [3, 4]. A high radiation dose increases the risk of side effects in organs at risk [1–3]. Thus, there is a limit to the number of allowable CBCT images due to the patient's radiation burden during treatment.

Accordingly, dose reduction is important and has been a major concern in reducing the risk of radiation poisoning. Various methods have been proposed to reduce the radiation dose from CBCT. These include decreasing the projection range using a collimator, rotating the x-ray source in different direction to avoid covering the critical organ, and reducing the scanning length, among others. However, these methods do not consider the size and shape of the patient.

To reduce the radiation dose given to patients, a tube current modulation (TCM) method has been widely used in diagnostic CT systems. This technique involves an adaptive tube current that is dependent on the integrated attenuation coefficient over a projection angle. This reduces the imaging dose while preserving optimal image quality [5–10]. Gies et al. [11, 12] have previously suggested an approach to apply TCM in CT by attenuating a body through a central axis to homogenize the noise by modulating X-ray intensities. Parsons et al. [13] have applied this TCM technique to a CBCT imaging system that included a four-blade dynamic kV collimator. This application was capable of reducing dose and image noise while providing high SNR values compared to those of conventional CBCT by adjusting fluence as a function of projection angle. However, due to limitations on the target imaging area, the technique could not easily confirm and revise the patient's position. In addition, information of the desired doses for particular image quality is not accessible.

A kV-CBCT acquires a volumetric image for a single rotation in order to confirm and revise the patient's position. Therefore, the TCM method has not yet been applied to a kV-CBCT system on a LINAC machine in a clinic. The purpose of this study is to investigate if a TCM method is desirable in kV-CBCT systems to confirm and revise the exact position of a patient for IGRT or not. We propose a framework for applying the developed TCM method to kV-CBCT systems.

To do so, we have developed an optimized attenuation–based TCM method using prior information from treatment planning CT images. This method provides an optimal radiation dose reduction without degrading image quality for kV-CBCT imaging. The proposed TCM method has been validated using both a numerical XCAT phantom and ATOM phantom. This framework has the potential to enable application of a TCM method in CBCT systems to reconstruct CT images of similar image quality to that of conventional methods while minimizing the total radiation dose. Thus, our study is expected to reduce the side effects of radiation exposure for patients in need of X-ray imaging.

Materials and methods

A. TCM framework

Patients were put through a diagnostic CT scan for RT planning. Using this information, one can estimate the total attenuation of an X-ray through a patient's body in a CBCT setting for radiation therapy. To apply the proposed TCM method to CBCT scans, previously scanned CT images for treatment planning were used as follows:

1. One slice of a treatment planning CT image that included the region of interest was chosen for processing.

2. Using Siddon's method [14], the amount of attenuation (A_i) for each projection was calculated in the chosen slice of a CT image.

3. The proposed TCM method calculated a minimum amount of current for each projection,

4. By applying the calculated TCM current for each projection, projection images were acquired and the CT image was reconstructed using a FDK algorithm.

We performed a numerical study incorporating major factors into account such as polychromatic X-rays, scatters, noise, and bow-tie filters in order to demonstrate that the TCM method can produce images of equivalent quality to that of CBCT using reduced imaging radiation doses [15]. The CT projector is a program provided with the XCAT phantom, which takes the numerical phantom as an input and generates projection data by angle. Using the CT projector program, 680 projection images of a XCAT phantom were obtained via a conventional scanning condition—i.e., without modulating the tube current—and the proposed TCM scanning condition for a simulation study. Alternatively, a patient's actual CT image of an ATOM phantom was used for an experimental study.

To generate a matrix of linear attenuation coeffients, we analyzed a 60 keV photon from the NIST because it was approximately within a mean energy of a 120 kVp spectrum of a X-ray tube on pelvis mode from a XVI-CBCT. Projection images were generated in 1˚ increments to achieve a full rotation around the phantom for both conventional CBCT and TCM scans.

B. Calculating the current of TCM to minimize radiation dose

Gies et al. studied the theoretical prediction of the TCM method, revealing that dose control via TCM has the potential to either improve image quality through noise reduction or reduce radiation exposure without impairing image quality [11]. Therefore, we developed a formulation based on that studied by Gies et al. to determine variations in fluence as a function of projection angle. Briefly, this calculation is described using the following equation from Gies et al.:

$$N_{0i} = \frac{N_0}{\sum_{i=1}^{P} \sqrt{A_i}} \cdot \sqrt{A_i} \qquad (1)$$

where N_{oi} is the required number of quanta after passing through the phantom at an angle i, N_o is the total number of emitted quanta throughout an acquisition (total current), P is the number of projections, and A_i is the amount of attenuation through the phantom at angle i. N_i is the number of quanta in view i, after traversing the object. Thus, the attenuation of the in-view, i, is given by $A_i = \frac{N_{0i}}{N_i}$.

Then, the pixel noise variance of the image without a TCM case is calculated using

$$\sigma^2 = \sum_{i=1}^{P} \sigma_i^2 = \sum_{i=1}^{P} \frac{A_i}{N_{0i}} \tag{2}$$

Substituting Eq (1) for Eq (2), the level of noise variance for a TCM-generated image is calculated using

$$\sigma^2 = \frac{\left(\sum_{i=1}^{P} \sqrt{A_i}\right)^2}{N_0} \tag{3}$$

From the above equations, we have devised a method that minimizes the total current for any given image quality using the TCM technique. To preserve an equivalent image quality to that of conventional CBCT, setting Eq (2) equal to Eq (3) yields Eq (4), as follows:

$$\sigma^2_{CBCT} = \sum_{i=1}^{P} \frac{A_i}{N_{0i}} = \frac{\left(\sum_{i=1}^{P} \sqrt{A_i}\right)^2}{N_0'} = \sigma^2_{TCM} \tag{4}$$

From this equation, the total current, N_o', could be generated to preserve image quality while minimizing dose, as follows:

$$N_0' = \frac{\left(\sum_{i=1}^{P} \sqrt{A_i}\right)^2}{\sum_{i=1}^{P} \frac{A_i}{N_{0i}}} \tag{5}$$

Finally, substituting Eq (5) for Eq (1), the minimized tube current, N_0', for each scanning angle can be written as Eq (6).

$$N_{0i}' = \frac{N_0'}{\sum_{i=1}^{P} \sqrt{A_i}} \sqrt{A_i} \tag{6}$$

Therefore, from the above equation, the method of minimizing the total current is finally derived to make a given image quality using the TCM technique. As Fig 1 shows, the amount of attenuation (A_i) was calculated in two ways: the central beam line attenuation was calculated and compared to the average attenuation over certain lines that were chosen by considering the beam shape on the detector.

C. Simulation study

C.1 OBI kV-CBCT system. The kV X-ray beams can be delivered in both half-fan and full-fan modes of a Varian on-board imager (OBI) system mounted on a linear accelerator [1, 16]. The full-fan mode is a default mode for the head-and-neck region because of its narrow field-of-view (FOV); whereas, the half-fan mode, due to its increased effective FOV size, is used for most other regions such as the chest, abdomen, and pelvis regions. For the simulation study, we used a pelvis mode with a half-fan mode. This scanning mode uses a half-fan bow-tie filter and a scanning angle of 360˚.

The pelvis mode was operated at its own default exposure condition, with a voltage of 125 kVp and a total current of 681 mAs. A schematic of the pelvis mode is shown in Fig 2. We have estimated the dose distribution and organ doses using a MC simulation for a conventional CBCT scan and TCM case, respectively.

The XCAT phantom, which is a realistic and flexible anatomical model of the whole human body for the study of medical imaging and an important tool for evaluating imaging devices

and techniques. In this study, the XCAT phantom was incorporated to calculate the absorbed radiation doses in organs at risk and validate the proposed TCM method for CBCT [17–20].

C.2 Monte carlo simulation. The organ dose due to imaging radiation has been calculated using the GATE v.6 simulation toolkit [21].

A Varian OBI kV-CBCT system was implemented according to system specifications. In addition, various radiation physics were included in this simulation such as the photoelectric effect, Compton scattering, Rayleigh scattering, electron ionization, Bremsstrahlung, and multiple scattering of electrons. The beam quality and quantity have been confirmed by comparing the weighted computed tomography dose index ($CTDI_w$) values reported outlined by the Varian Medical Systems [22, 23].

D. Experimental study

D.1 XVI kV-CBCT system. Our Elektra System has a XVI CBCT system (Elekta, Crawley, UK) [2, 4]. There were two filter cassettes available for the unit: the F0 neutral filter and F1
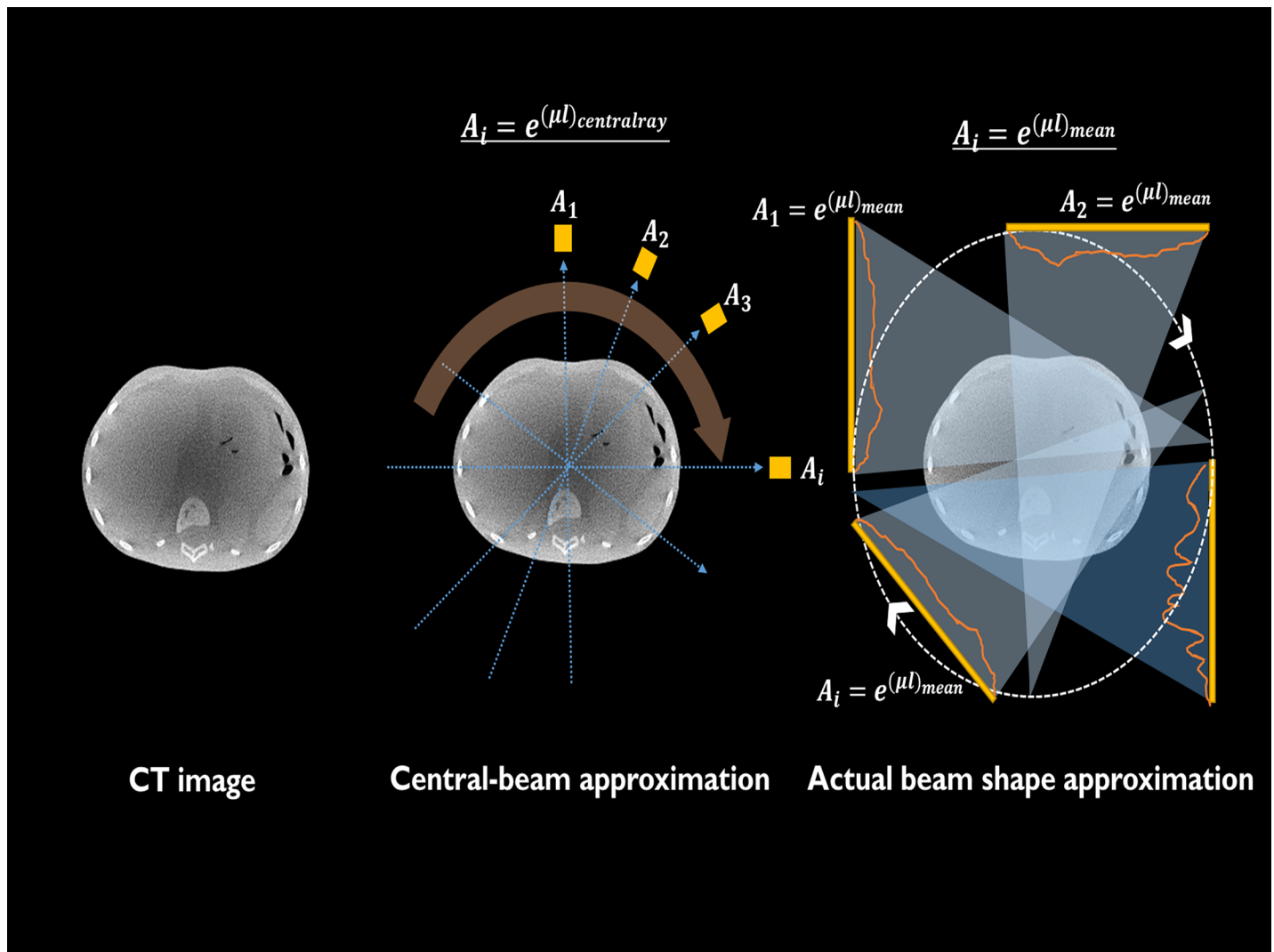

Fig 1. Framework for calculating Ai values. After selecting the CT image as in (a), we calculated the Ai value by two methods (b) Central-beam approximation and (c) actual beam shape approximation.
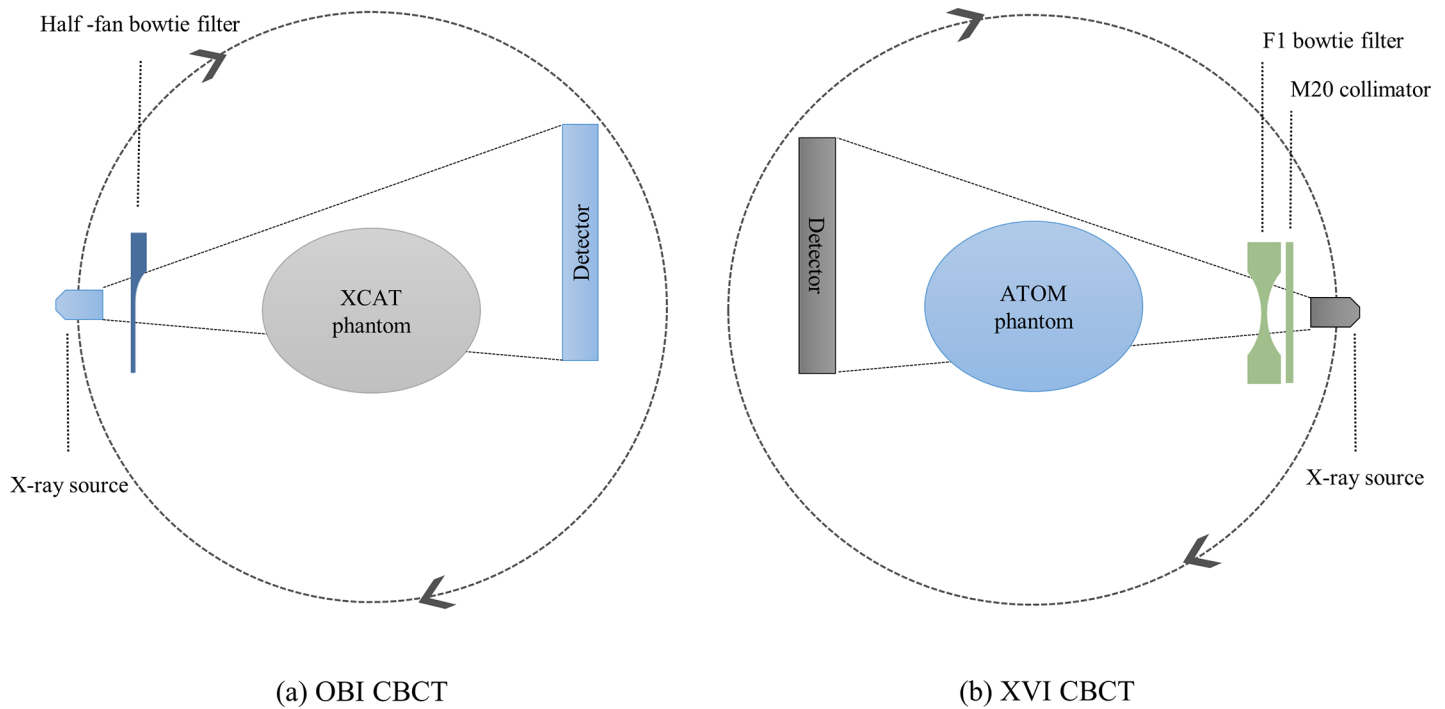
Fig 2. Half-fan scanning geometry. (a) OBI CBCT and (b) XVI CBCT system. The default detector position shifted 14.8 cm using the OBI and 11.5 cm for the XVI in medium-FOV mode.

bowtie filter. All cassettes had thin plastic windows at the top and bottom. The F1 bowtie filter was made of an aluminum alloy, and the shape of the bowtie was doubly concave in the cross-line direction and flat about the central beam axis in the inline direction.

There were also three types of collimator cassettes used: Small, Medium, and Large. Each type produced a small, medium, or large field of view (FOV), respectively, wherein the different FOVs were defined by the panel offset from the central axis of the kV. The F1 and M20 filter cassette and collimator type, respectively, were used in this study. The pelvis scan mode in the XVI—whose default projection conditions were given as 120kVp, 3.125 mAs—was adopted for 360 projection views per angle in this study.

D.2 The ATOM phantom. CIRS ATOM phantoms are a full line of anthropomorphic, cross-sectional dosimetry phantoms designed to investigate organ dose, whole body effective dose, and evaluate image quality [24]. We selected the adult male phantom for this study. This phantom is sectional in design, with traditional 25 mm thick sections. Fig 3 shows the XVI CBCT and ATOM phantom.

Results

A. Simulation results

In Fig 4, the optimum TCM current for each projection angle was plotted for the XCAT's abdominal region. The current was modulated for each projection angle to provide more current for higher attenuation angles and less current for lower attenuation angles.

Fig 5 shows a conventional CBCT image and TCM image for both central and off-center slices. Although the total amount of current for the TCM image was reduced by 21% compared to the conventional image, there was little difference between the reconstructed images. The normalized root-mean square error (NRMSE) and structure similarity (SSIM) index were

Fig 3. The Elekta XVI-CBCT system and CIRS ATOM phantom.

calculated to investigate the quantitative accuracy of the images. The NRMSE used in this study was defined by

$$\text{NRMSE} = \mu^{-1}\sqrt{\frac{1}{N}\sum_{i=1}^{N}(x_i - \mu)^2} \qquad (7)$$

where μ is mean value of the ROI; x_i signified the pixel values in the ROI; and N is the number
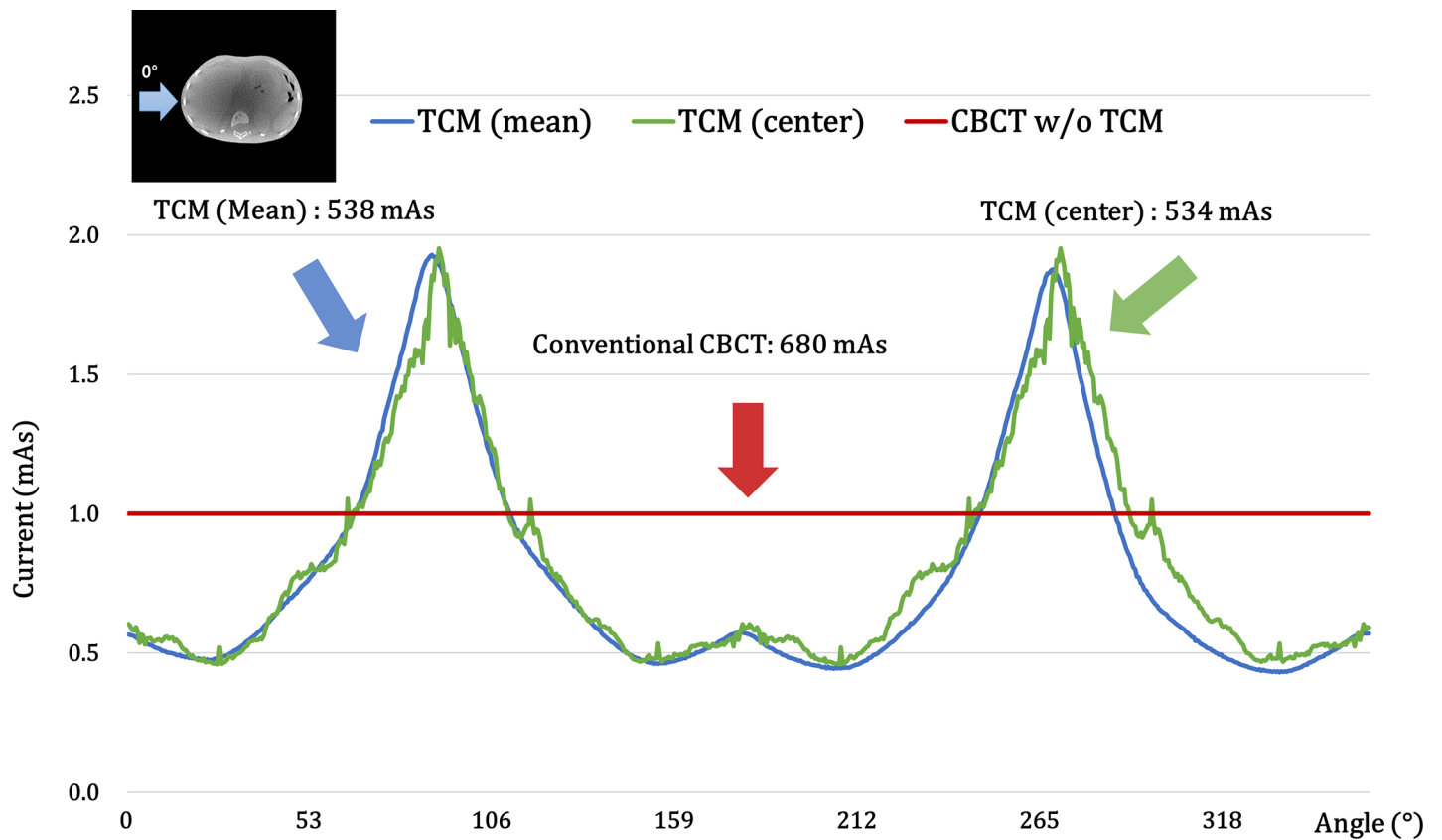

Fig 4. TCM dose per angle for simulation study. The red line shows a conventional CBCT scan, the green-line represents a TCM scan from a center-beam approximation, and the blue-line indicates a TCM scan of an actual beam shape approximation.
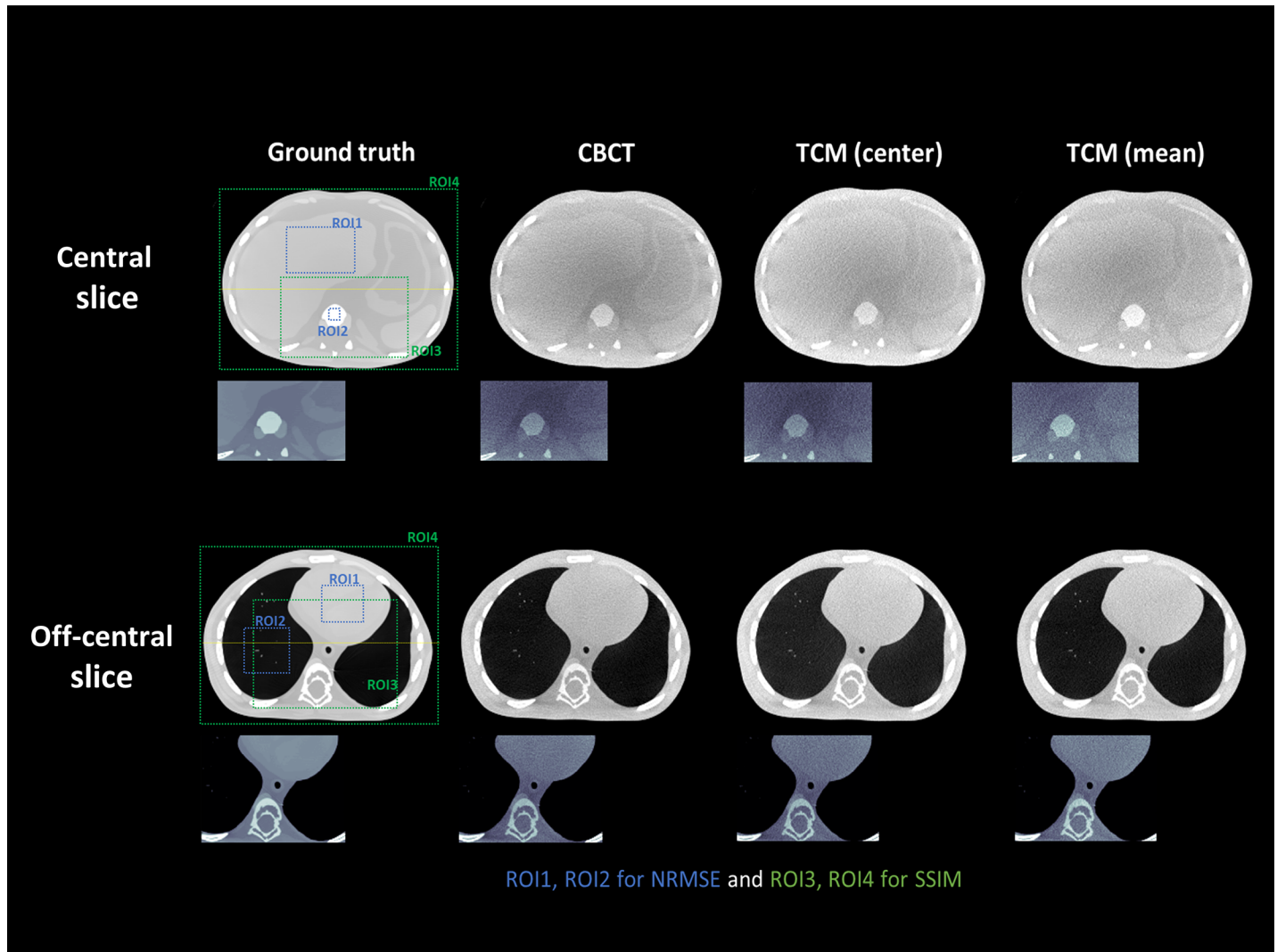
Fig 5. Reconstructed images of the XCAT phantom for central and off-center slices from conventional CBCT and TCM methods.

of pixels within the ROI. A structure similarity index was used to measure the degree of similarity between the reference image and an image of interest. The SSIM is sensitive to contrast, luminance, and structures within an image. Its value ranges from 0 to 1. As the SSIM value gets closer to 1, the similarity between the reference and image of interest increases [25]. Table 1 shows reconstructed CT images using the TCM method had comparable NRMSE properties and similar SSIM values to the reference images acquired via conventional CBCT at both central and off-center slices. In addition, the reconstructed TCM images exhibited small difference between the central beam approximation and actual beam shape approximation. Reconstructed images from the actual beam shape approximation had similar values to those from a conventional method.

B. Calculating organ dose

The imaging doses for abdominal and pelvic organs are shown in Fig 6. Using the TCM scans in the pelvis mode, a reduction in organ doses ranged from 14% to 31% in comparison to

Table 1. NRMSE and SSIM values are calculated for center and off-center slices. ROIs are defined in Fig 5.

Center slice	NRMSE		SSIM	
	ROI1 (tissue)	ROI2 (bone)	ROI3	ROI4 (all)
Ground	0.0112	0.0037	-	-
CBCT	0.0686	0.0396	0.9875	0.9997
TCM_center	0.0740	0.0427	0.9866	0.9996
TCM_mean	0.0691	0.0404	0.9943	0.9999
Off-center slice	NRMSE		SSIM	
	ROI1 (heart)	ROI2 (lung)	ROI3	ROI4 (all)
Ground	0.0240	0.0680	-	-
CBCT	0.0449	0.0978	0.9989	0.9995
TCM_center	0.0483	0.1051	0.9989	0.9995
TCM_mean	0.0449	0.1047	0.9995	0.9997

conventional CBCT scans. The organ doses were calculated to range from 2.67 to 3.69 cGy for the conventional CBCT scan, and 1.95 to 2.97 cGy for the TCM scan. Those from the TCM scans were around 20% lower for abdominal organs and 29% lower for pelvic organs when compared to the conventional CBCT mode.
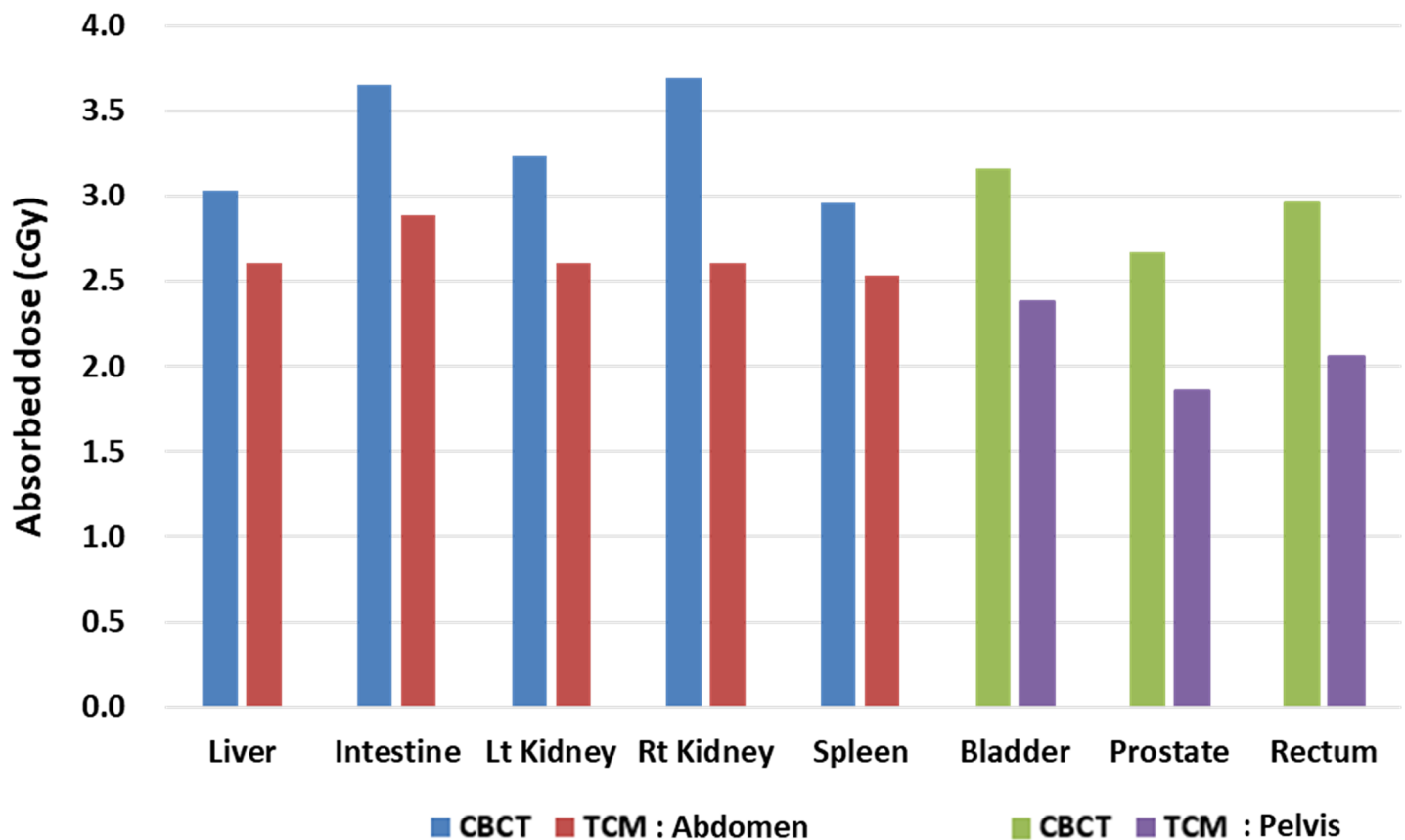

Fig 6. Imaging dose to abdominal and pelvic organs from conventional CBCT and TCM scans using a XCAT phantom.
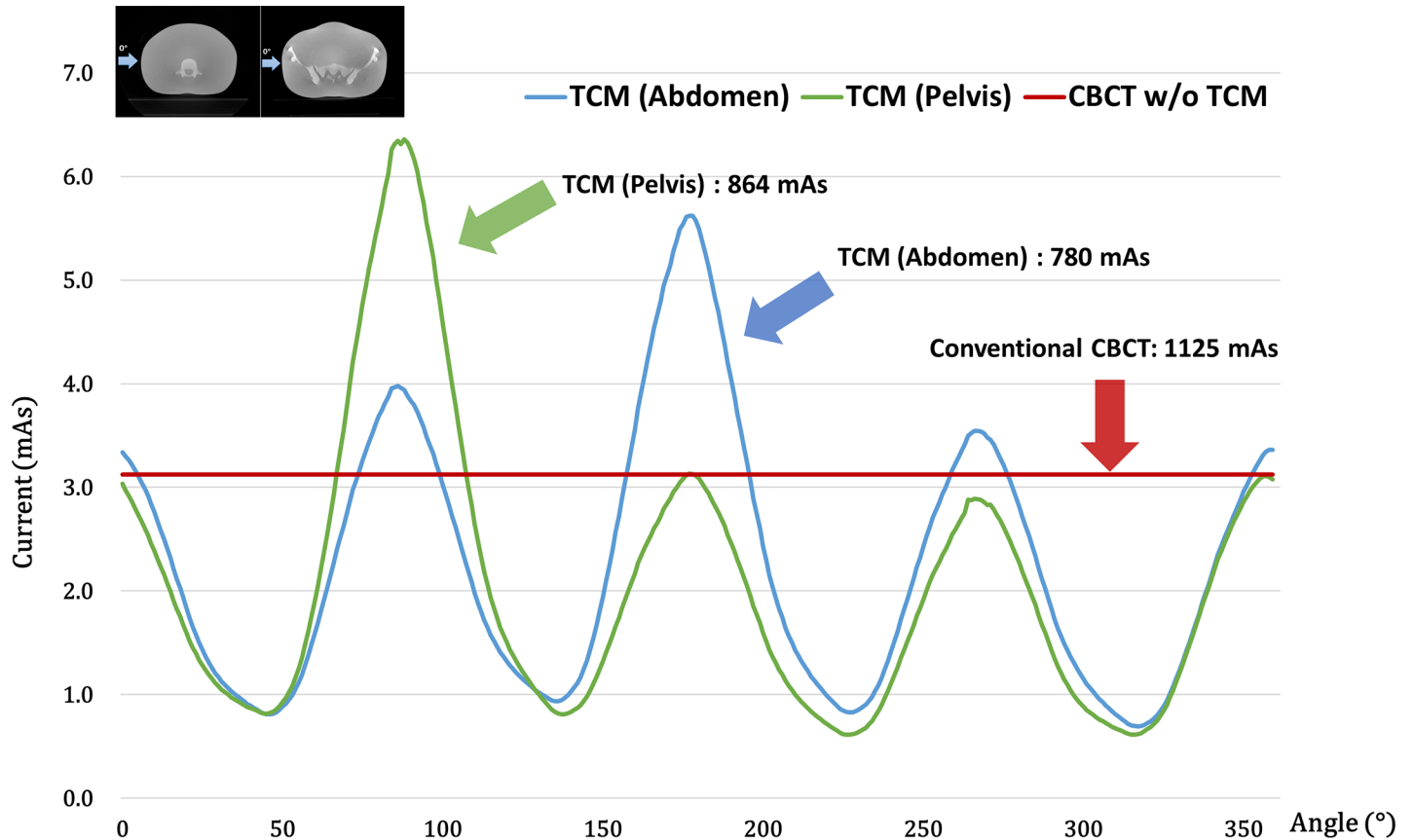
Fig 7. TCM dose per angle is calculated for the abdominal and pelvic regions of the ATOM phantom. The red line shows the results of a conventional CBCT scan; the green line represents the TCM scan of the pelvic region; and the blue line signifies the TCM scan of the abdominal region.

https://doi.org/10.1371/journal.pone.0192933.g007

C. Experimental results

In Fig 7, we calculated the optimal TCM current and projection angle for the ATOM abdominal and pelvic regions shown in Fig 1. We conducted an experimental study using TCM to get an actual beam shape approximation. As shown in the simulation study, variations in the amount of current along with projection angle were observed. Compared with a symmetrically current-modulated abdominal region, we found asymmetry in the pelvic region due to the greater number of bones in this region.

Fig 8 shows a conventional CBCT image and TCM image of an ATOM abdominal region for central and off-center slices. Although the total dose for the TCM image was reduced by 23% compared with that of the conventional image, both images exhibited comparable image quality for image guidance. The line profiles for the dashed lines in Fig 8 are shown in Fig 9. The line profile of the reconstructed image using the TCM method is plotted as a dash-dot red line. The TCM image had a similar value to that of the conventional CBCT image.

As shown in Table 2, there is little difference in terms of NRMSE values for soft tissue and bone between the TCM and conventional images. SSIM values of the selected ROIs were very close to 1. Moreover, the reconstructed images of the ATOM pelvic region from conventional CBCT and the TCM method are shown in Fig 10. Here, the three parts comprise the central slice, off-center slice of the upper region, and off-center slice of the lower region. Even though the total dose for the TCM image was reduced by 31%, the image itself was a little noisier than
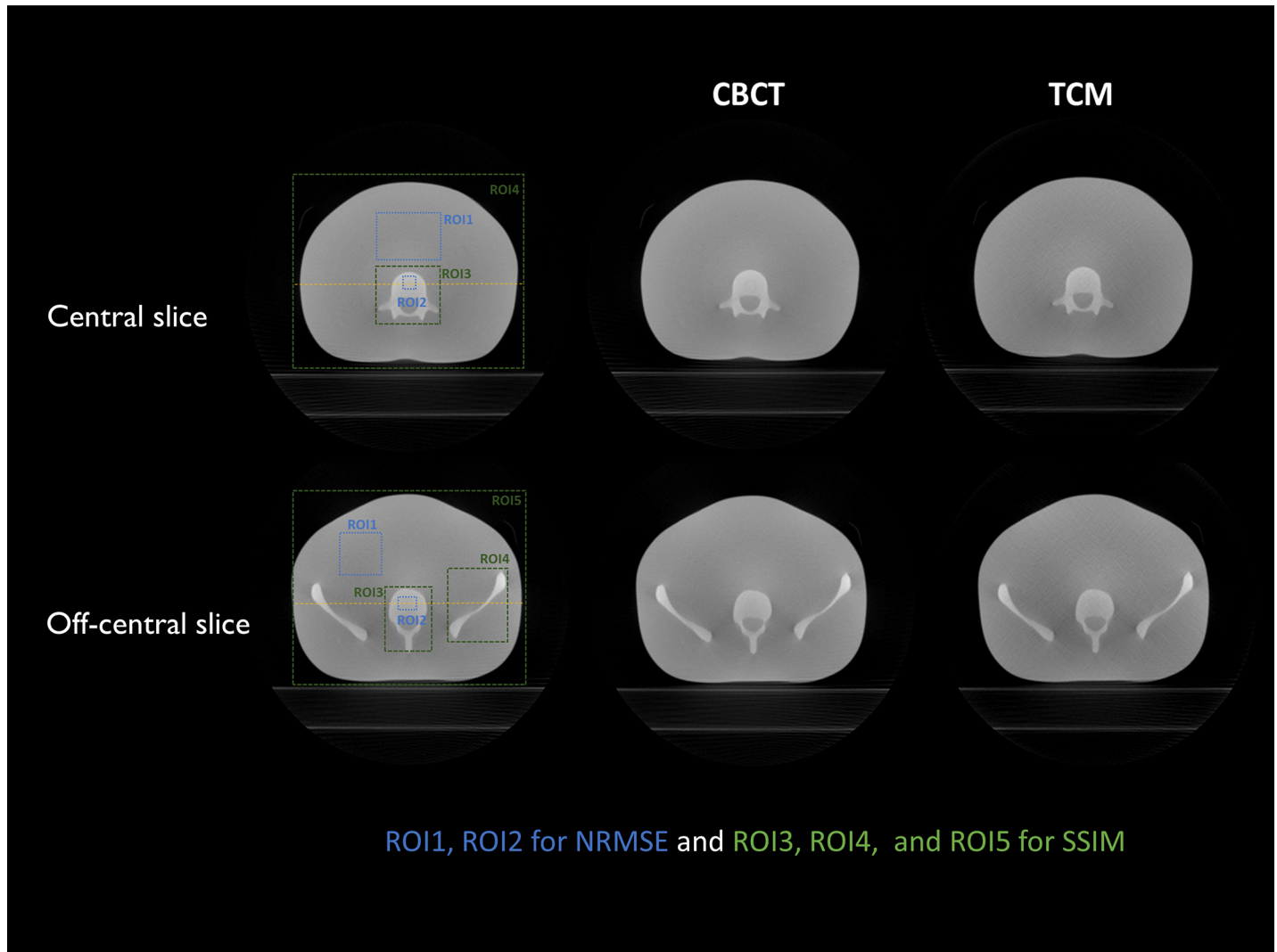
Fig 8. Reconstructed images of the ATOM's abdominal region using conventional CBCT and TCM methods. XVI images are obtained via central and off-center slices.

the CBCT image, but the detailed structures were similar. The quantitative evaluation in Table 3 shows that NRMSE values of the TCM exhibited little difference when compared with those of the CBCT. SSIM values confirmed that the TCM image was comparable to the conventional CBCT image.

Discussion

Gies et al. [11] have previously described a method to calculate TCM in CT based on the attenuation through a central axis, resulting in a desired number of quanta at the detector plane for every projection. This shows that both dose and image noise could be reduced. To the best of our knowledge, there is no precedent where this TCM method is applied to a CBCT system for clinical applications.

Parsons et al. [13] recently showed that the TCM method could be successfully applied to kV-CBCT using a collimator to image the target region. Doing so demonstrated a reduction in
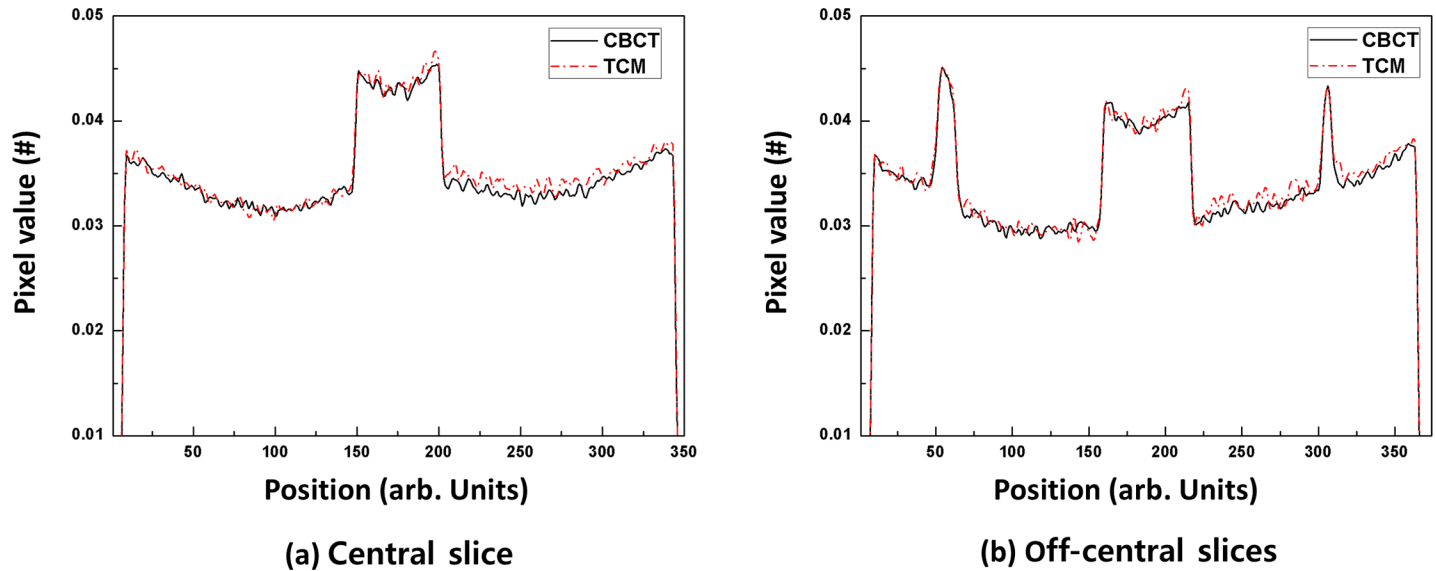
(a) Central slice   **(b) Off-central slices**

Fig 9. Line profiles from Fig 8. A conventional CBCT image is plotted as a solid black line; the TCM images are plotted as dash-dot red lines.

noise values compared to those from conventional kV-CBCT. However, due to a limited target area, there were limitations in the ability to confirm and revise the patient's position. Moreover, proper dose information to yield high image quality has not been accessible.

In our study, we calculated the amount of attenuation for each projection angle, taking into account the actual beam shape of the CBCT, based on the patient's CT image. We then reconstructed the image for a desired image quality, without truncation. To do so, we calculated the minimum amount of TCM current needed to reconstruct an image with our desired quality. The results indicate that the proposed TCM method yielded comparable image quality to that from conventional CBCT images, while organ doses were significantly lower using TCM. Thus, radiation risk could be decreased by minimizing the required dose needed to reconstruct a CBCT image.

The potential to apply TCM in a CBCT system was demonstrated with our proposed framework. We used a previously acquired plan CT images for the TCM method so that additional radiation exposure could be avoided. We also calculated patient-specific TCM currents based on attenuation. We reconstructed the entire area of each image rather than a partially targeted area, thereby increasing clinical efficiency.

Our study can be applied not only to kV-CBCT on LINAC for radiation therapy, but also to C-arm CT for interventional radiology. However, the proposed method requires a CT image taken in advance to obtain the tube current by angle. Maybe it is possible to modulate the beam current based on the patient's size and shape which wouldn't require an input CT image.

Table 2. NRMSE and SSIM are calculated for center and off-center slices. ROIs are defined in Fig 8.

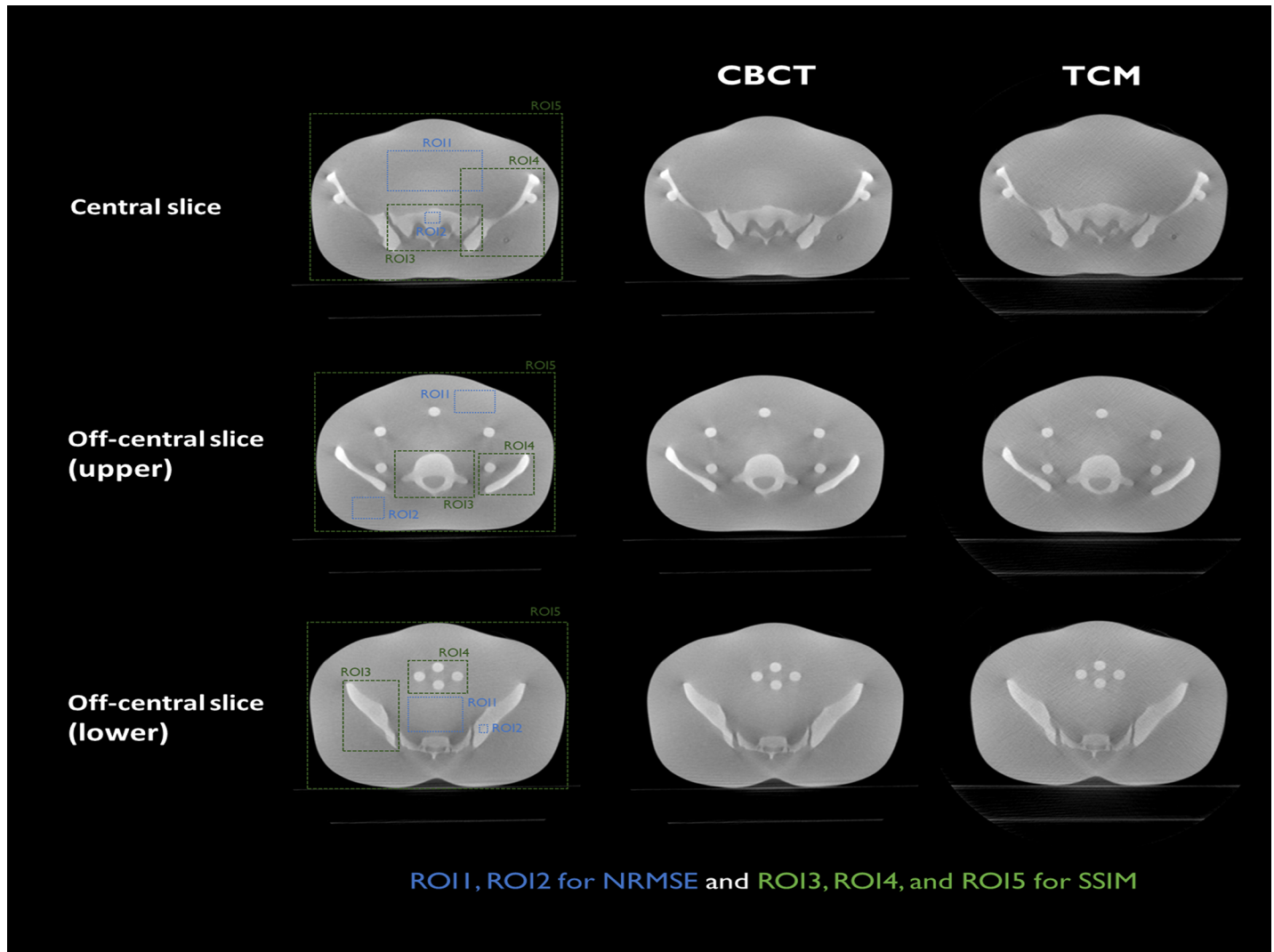| ATOM Abdomen		Center slice		Off-center slice		
		ROI1 (tissue)	ROI2 (bone)	ROI1 (tissue)	ROI2 (bone)	
NRMSE	CBCT	0.0192	0.0315	0.0212	0.0247	
	TCM	0.0207	0.0329	0.0219	0.0266	
		ROI3 (bone)	ROI4 (all)	ROI3 (bone1)	ROI4 (bone2)	ROI5 (all)
SSIM	TCM	0.9996	0.9999	0.9998	0.9999	0.9999

Fig 10. Reconstructed images of ATOM's pelvic region from conventional CBCT and TCM methods. XVI images are from the central, upper, and lower off-center regions.

https://doi.org/10.1371/journal.pone.0192933.g010

We chose the central slice as our region of interest and calculated the TCM dose based on a central beam approximation or actual beam-shape approximation. In the future, we will calculate the TCM dose based on a CBCT 3D volumetric beam shape to improve the accuracy of the TCM image. Furthermore, we believe that combining this technique with noise reduction or iterative reconstruction algorithms would yield great improvements to the TCM image [2, 26–28].

Table 3. NRMSE and SSIM calculated for central and off-center slices. ROIs are defined in Fig 10.

ATOM Abdomen		Center slice			Off-center slice (upper)			Off-center slice (lower)		
		ROI1 (tissue)	ROI2 (bone)		ROI1 (center)	ROI2 (side)		ROI1 (tissue)	ROI2 (bone)	
NRMSE	CBCT	0.0308	0.0304		0.0161	0.0182		0.0495	0.0160	
	TCM	0.0309	0.0302		0.0171	0.0185		0.0505	0.0155	
		ROI3 (bone1)	ROI4 (bone2)	ROI5 (all)	ROI3 (bone1)	ROI4 (bone2)	ROI5 (all)	ROI3 (bone1)	ROI4 (bone2)	ROI5 (all)
SSIM	TCM	0.9977	0.9984	0.9999	0.9984	0.9971	0.9997	0.9962	0.9952	0.9997

https://doi.org/10.1371/journal.pone.0192933.t003

Conclusions

We have successfully demonstrated the feasibility and dosimetric merit of a TCM method for kV-CBCT via simulation and experimental study. The results substantiate the idea that the proposed TCM method and framework can be a useful option for CBCT imaging that provides optimized dose reductions without degrading image quality. Therefore, the probability for side effects due to radiation exposure can be significantly decreased.

Author Contributions

Conceptualization: Kihong Son, Jieun Chang, Seungryong Cho, Jin Sung Kim.

Data curation: Kihong Son, Jieun Chang, Changhwan Kim, Sohyun Park.

Formal analysis: Kihong Son, Jieun Chang, Hoyeon Lee.

Funding acquisition: Seungryong Cho, Jin Sung Kim.

Methodology: Kihong Son, Jieun Chang, Seungryong Cho.

Software: Kihong Son, Hoyeon Lee, Taewon Lee.

Supervision: Seungryong Cho, Jin Sung Kim.

Validation: Kihong Son, Jieun Chang.

Writing – original draft: Kihong Son.

Writing – review & editing: Kihong Son, Seungryong Cho, Jin Sung Kim.

References

1. Son K, Cho S, Kim JS, Han Y, Ju SG, Choi DH. Evaluation of radiation dose to organs during kilovoltage cone-beam computed tomography using Monte Carlo simulation. Journal of applied clinical medical physics. 2014; 15(2):4556. https://doi.org/10.1120/jacmp.v15i2.4556 PMID: 24710444

2. Alaei P, Spezi E. Imaging dose from cone beam computed tomography in radiation therapy. Phys Medica. 2015; 31(7):647–58.

3. Ding GX, Munro P, Pawlowski J, Malcolm A, Coffey CW. Reducing radiation exposure to patients from kV-CBCT imaging. Radiother Oncol. 2010; 97(3):585–92. https://doi.org/10.1016/j.radonc.2010.08.005 PMID: 20846736

4. Hyer DE, Serago CF, Kim S, Li JG, Hintenlang DE. An organ and effective dose study of XVI and OBI cone-beam CT systems. Journal of applied clinical medical physics. 2010; 11(2):181–97.

5. Greess H, Nomayr A, Wolf H, Baum U, Lell M, Bowing B, et al. Dose reduction in CT examination of children by an attenuation-based on-line modulation of tube current (CARE Dose). European radiology. 2002; 12(6):1571–6. https://doi.org/10.1007/s00330-001-1255-4 PMID: 12042970

6. Greess H, Wolf H, Baum U, Lell M, Pirkl M, Kalender W, et al. Dose reduction in computed tomography by attenuation-based on-line modulation of tube current: evaluation of six anatomical regions. European radiology. 2000; 10(2):391–4. https://doi.org/10.1007/s003300050062 PMID: 10663775

7. Kalra MK, Maher MM, Toth TL, Schmidt B, Westerman BL, Morgan HT, et al. Techniques and applications of automatic tube current modulation for CT. Radiology. 2004; 233(3):649–57. https://doi.org/10.1148/radiol.2333031150 PMID: 15498896

8. McCollough CH, Primak AN, Braun N, Kofler J, Yu LF, Christner J. Strategies for Reducing Radiation Dose in CT. Radiol Clin N Am. 2009; 47(1):27–+. https://doi.org/10.1016/j.rcl.2008.10.006 PMID: 19195532

9. Rizzo S, Kalra M, Schmidt B, Dalal T, Suess C, Flohr T, et al. Comparison of angular and combined automatic tube current modulation techniques with constant tube current CT of the abdomen and pelvis. Am J Roentgenol. 2006; 186(3):673–9.

10. Soderberg M, Gunnarsson M. Automatic exposure control in computed tomography—an evaluation of systems from different manufacturers. Acta Radiol. 2010; 51(6):625–34. https://doi.org/10.3109/02841851003698206 PMID: 20429764

11. Gies M, Kalender WA, Wolf H, Suess C. Dose reduction in CT by anatomically adapted tube current modulation. I. Simulation studies. Medical physics. 1999; 26(11):2235–47. https://doi.org/10.1118/1.598779 PMID: 10587204

12. Kalender WA, Wolf H, Suess C. Dose reduction in CT by anatomically adapted tube current modulation. II. Phantom measurements. Medical physics. 1999; 26(11):2248–53. https://doi.org/10.1118/1.598738 PMID: 10587205

13. Parsons D, Robar JL. Volume of interest CBCT and tube current modulation for image guidance using dynamic kV collimation. Medical physics. 2016; 43(4):1808–17. https://doi.org/10.1118/1.4943799 PMID: 27036578

14. Siddon RL. Fast calculation of the exact radiological path for a three-dimensional CT array. Medical physics. 1985; 12(2):252–5. https://doi.org/10.1118/1.595715 PMID: 4000088

15. Sun M, Star-Lack JM. Improved scatter correction using adaptive scatter kernel superposition. Phys Med Biol. 2010; 55(22):6695–720. https://doi.org/10.1088/0031-9155/55/22/007 PMID: 21030750

16. Ding GX, Munro P. Radiation exposure to patients from image guidance procedures and techniques to reduce the imaging dose. Radiother Oncol. 2013; 108(1):91–8. https://doi.org/10.1016/j.radonc.2013.05.034 PMID: 23830468

17. Paul Segars W, Tsui BM. MCAT to XCAT: The Evolution of 4-D Computerized Phantoms for Imaging Research: Computer models that take account of body movements promise to provide evaluation and improvement of medical imaging devices and technology. Proceedings of the IEEE Institute of Electrical and Electronics Engineers. 2009; 97(12):1954–68. https://doi.org/10.1109/JPROC.2009.2022417 PMID: 26472880

18. Segars WP, Mahesh M, Beck TJ, Frey EC, Tsui BMW. Realistic CT simulation using the 4D XCAT phantom. Medical physics. 2008; 35(8):3800–8. https://doi.org/10.1118/1.2955743 PMID: 18777939

19. Segars WP, Sturgeon G, Mendonca S, Grimes J, Tsui BM. 4D XCAT phantom for multimodality imaging research. Medical physics. 2010; 37(9):4902–15. https://doi.org/10.1118/1.3480985 PMID: 20964209

20. Panta RK, Segars P, Yin FF, Cai J. Establishing a framework to implement 4D XCAT Phantom for 4D radiotherapy research. J Cancer Res Ther. 2012; 8(4):565–70. https://doi.org/10.4103/0973-1482.106539 PMID: 23361276

21. Jan S, Benoit D, Becheva E, Carlier T, Cassol F, Descourt P, et al. GATE V6: a major enhancement of the GATE simulation platform enabling modelling of CT and radiotherapy. Phys Med Biol. 2011; 56(4):881–901. https://doi.org/10.1088/0031-9155/56/4/001 PMID: 21248393

22. Kim S, Yoshizumi T, Toncheva G, Yoo S, Yin FF, Frush D. Estimation of Computed Tomography Dose Index in Cone Beam Computed Tomography: Mosfet Measurements and Monte Carlo Simulations. Health Phys. 2010; 98(5):683–91. https://doi.org/10.1097/HP.0b013e3181cd3ec3 PMID: 20386198

23. Varian Medical Systems. Varian On-Board Imager (OBI) Reference Guide. Palo Alto (CA): Varian Medical Systems, 17071 (2008).

24. Zhang D, Li XH, Gao YM, Xu XG, Liu B. A method to acquire CT organ dose map using OSL dosimeters and ATOM anthropomorphic phantoms. Medical physics. 2013; 40(8).

25. Wang Z, Bovik AC, Sheikh HR, Simoncelli EP. Image quality assessment: from error visibility to structural similarity. IEEE transactions on image processing: a publication of the IEEE Signal Processing Society. 2004; 13(4):600–12.

26. Cho S, Lee T, Min J, Chung H. Feasibility study on many-view under-sampling technique for low-dose computed tomography. Opt Eng. 2012; 51(8). https://doi.org/10.1117/1.OE.51.8.080502 PMID: 24058220

27. Cho SY, Pearson E, Pelizzari CA, Pan XC. Region-of-interest image reconstruction with intensity weighting in circular cone-beam CT for image-guided radiation therapy. Medical physics. 2009; 36(4):1184–92. https://doi.org/10.1118/1.3085825 PMID: 19472624

28. Abbas S, Lee T, Shin S, Lee R, Cho S. Effects of sparse sampling schemes on image quality in low-dose CT. Medical physics. 2013; 40(11):111915. https://doi.org/10.1118/1.4825096 PMID: 24320448